SF2A 2007
J. Bouvier, A. Chalabaev, C. Charbonnel (eds)

INHOMOGENEOUS EXTRAGALACTIC MAGNETIC FIELDS AND THE SECOND KNEE IN THE COSMIC RAY SPECTRUM

K. Kotera[1] and M. Lemoine[1]

Abstract. Various experiments indicate the existence of a second knee around energy $E = 3 \times 10^{17}$ eV in the cosmic ray spectrum. This feature could be the signature of the end of the galactic component and of the emergence of the extragalactic one, provided that the latter cuts off at low energies. Recent analytical calculations have shown that this cut-off could be a consequence of the existence of extragalactic magnetic fields (Lemoine 2005; Aloisio & Berezinsky 2005): low energy protons diffuse on extragalactic magnetic fields and cannot reach the observer within a given time. We study the influence of inhomogeneous magnetic fields on the magnetic horizon, using a new semi-analytical propagation code. Our results indicate that, at a fixed value of the volume averaged magnetic field $\langle B \rangle$, the amplitude of the low energy cut- off is mainly controled by the strength of magnetic fields in the voids of the large scale structure distribution.

1 Introduction

One observes three outstanding features in the high energy part of the cosmic ray spectrum: the knee around $E \sim 10^{15}$ eV, the second knee around $E \sim 3 \times 10^{17}$ eV and the ankle at $E \sim 10^{19}$ eV. One elegant way to explain these features is the 'dip model' (Berezinsky et al. 2002), in which the second knee is obtained by the cross-over between the galactic and the extragalactic components, the ankle being a propagation effect. It is notoriously difficult to accelerate particles beyond $E \sim 10^{15}$ eV in supernovae remnants (Lagage & Cesarsky 1983). This point constitutes the flaw of the traditional interpretation, in which the ankle is associated with the emergence of an extragalactic component, and the success of the 'dip model'.

This model still has its own drawbacks, the major one being its dependency on the cosmic ray chemical composition. It has indeed been argued that if ultra high energy cosmic rays comprised a significant fraction of heavy nuclei (more than $\sim 15\,\%$), the dip induced by energy losses would no longer reproduce the observed ankle feature. While we wait for the forthcoming cosmic ray composition measurement results, we will assume in the following discussion the validity of the 'dip model'.

Another point that had to be investigated in the original scenario of Berezinsky et al. (2002), was the reason why the extragalactic component vanishes at energies below the second knee. Lemoine (2005) and Aloisio & Berezinsky (2005) demonstrated that this cut-off could be tightly related to extragalactic magnetic fields. They demonstrated that if the intensity of extragalactic magnetic fields is rather modest, say $\langle B \rangle \sim 10^{-9}\,\mathrm{G}$, the diffusion time of particles with energy $E \leq 10^{17}\,\mathrm{eV}$ from the closest sources (located at, say $\sim 50 - 100\,\mathrm{Mpc}$) becomes longer than the age of the Universe. This produces a low energy cut-off in the propagated spectrum at the required location, which allows to reproduce a smooth transition at the second knee in agreement with observational data (see Lemoine 2005).

Quantizing the influence of extragalactic magnetic fields on the spectrum of cosmic rays with energy $E \sim 10^{17}\,\mathrm{eV}$ is not an easy task as the propagation times become of the order of a Hubble time, hence one must account for the effects of expansion. For the sake of simplicity, Lemoine (2005) and Aloisio & Berezinsky (2005) have thus assumed the magnetic field power to be distributed homogeneously in space. However, this approximation deserves to be refined since the magnetic field is most likely distributed as the charged baryonic plasma. Since the scale of inhomogeneity of large scale structure in the Universe is comparable to the distance

[1] Institut d'Astrophysique de Paris, UMR 7095 - CNRS, Université Pierre & Marie Curie, 98 bis boulevard Arago, F-75014 Paris, France

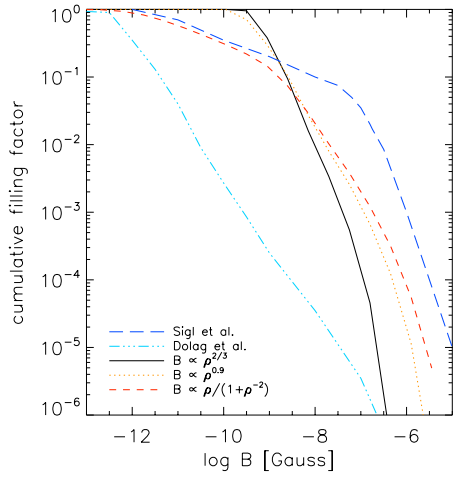

Fig. 1. Volume filling factor of the magnetic field in different scenarios. In dot-dashed line, the magnetic field simulated by Dolag and coauthors (2005); in long-dashed line, that simulated by Sigl and coauthors (2004). In solid line, the semi-analytic model with $B \propto \rho^{2/3}$, in orange dotted line, $B \propto \rho$. In red dashed line, the model $B \propto \rho \left[1 + (\rho/\overline{\rho})^{-2}\right]$; this model simulates a volume with unmagnetized voids. In all cases the proportionality factor $B_0 = 2$ nG.

to the closest sources, $\sim 50 - 100$ Mpc, the inhomogeneity of the magnetic field may affect the conclusions of Lemoine (2005) and Aloisio & Berezinsky (2005). The objective of the present paper is precisely to address this issue and to study the scenario put forward in these references in a more realistic extragalactic magnetic field configuration.

It is of course impossible to conduct such a study through analytical calculations. As a by-product of the present study, we thus propose a simple and new recipe to build semi-realistic magnetic field distributions out of dark matter simulations (which can be obtained at a lesser cost than MHD numerical simulations) as well as a new transport scheme which is more efficient than existing codes in several respects.

The paper is organized as follows. In Section 2, we present our recipes for magnetic field modeling and for cosmic ray transport. In Section 3 we address the issue of the low energy cut-off in various models of extragalactic magnetic fields distributions, compute the spectra and compare them to experimental data. Section 4 presents some observable signatures derived from our simulations. Finally, Section 5 summarizes our findings.

2 A new semi-analytical particle propagation code

Several pioneering works have studied the propagation of cosmic rays in so-called "realistic" magnetized environments (Dolag et al. 2005; Sigl et al. 2004). Figure 1 presents the volume filling factors of the magnetic field strength obtained in these MHD numerical simulations (the model of Dolag et al. (2005) is shown as the dot-dashed line, while the model of Sigl et al. (2004) is given by the long-dashed line). It reveals large differences in the volume averaged magnetic field as well as in the spatial distribution of these fields (which translates in this figure as a difference in the slopes of the volume filling factor). The origin of this difference is not understood and indicates the need for alternative methods to study the transport of high energy cosmic rays in extragalactic magnetic fields, in order to provide new angles of attack on this difficult problem. This constitutes one major motivation of the present work, in which we develop one such method and apply it to the study of the low energy cut-off at energies close to the second knee.

Our magnetized volume is constructed in a simple way as compared to Dolag et al. (2005) and Sigl et al. (2004), this simplicity offering various advantages (and admittedly, several drawbacks) as discussed in Kotera & Lemoine (2007). The core of our method is to map the magnetic field strength over the gas density using an analytical relation $B(\rho)$ (to be specified later) and to distribute randomly the magnetic field orientation in cells of coherence length l_c. The gas density itself is obtained from a high resolution dark matter numerical simulation of large scale structure formation (with standard cosmological parameters $\Omega_\Lambda = 0.7$, $\Omega_m = 0.3$ and $H_0 = 70\,\mathrm{km/s/Mpc}$). Once the volume has been set up, cosmic ray trajectories are simulated as follows. At each step, the cosmic ray is supposed to enter a spherical cell of coherence of the magnetic field defined by its diameter l_c, in which the magnetic field orientation is random. The time spent in the cell and the direction of exit of the cosmic ray are then drawn from semi-analytic distributions which simulate the transport of the

particle in MHD turbulence, according to studies carried out in Casse et al. (2002). The particle is then moved to another coherent cell and the next step is simulated. As we explain in Section 3, we finally compute the propagated spectrum in the low energy region $E \leq 10^{17}$ eV in a semi-analytic way which allows us to model the effect of cosmological expansion over the course of propagation from the source to the detector. In detail, we use the Monte Carlo simulations of particle propagation in the extragalactic magnetic fields at zero redshift in order to measure the diffusion coefficients, and use existing analytical formulae in order to calculate the propagated spectra from the diffusion equation in an expanding space-time. More details on this latter step are provided in Section 3.

We map the magnetic field over the matter density field using three laws:

$$B \propto \rho^{2/3} , \tag{2.1}$$

$$B \propto \rho^{0.9} \tag{2.2}$$

$$B \propto \rho \left[1 + \left(\frac{\rho}{\langle \rho \rangle} \right)^{-2} \right] . \tag{2.3}$$

The first and second laws can be analytically derived in the case respectively of an isotropic and an anisotropic collapse of structures. The last model is an ad-hoc modeling of the suppression of magnetic fields in the voids of large structure which leaves unchanged the distribution in the dense intergalactic medium (meaning $\rho > \langle \rho \rangle$). These models account for dynamo and shear effects that occur during the magnetic field amplification, up to some extent, as they reproduce the characteristic features obtained in the numerical simulations that include those effects. The choice of a random orientation of the magnetic field in each coherence cell also neglects the influence of large scale motions.

3 Results

The following results were obtained by computing the trajectories of 10^3 protons in inhomogeneous magnetic fields mapped according to four models, for many sets of energies E, magnetic field characteristic values B_0 and coherence lengths l_c. We will label in what follows "models 1−3" our modeling of $B(\rho)$ presented in Eqs. (2.1−2.3). We add to these models a last one (model 4) for which $B \propto \rho^{2/3}$ and the level of turbulence $\eta = \langle \delta B^2 \rangle / \langle B^2 \rangle \ll 1$, where δB is the inhomogeneous perturbation component of B (defined such as: $B = \langle B \rangle + \delta B$). Though B_0 and $\langle B \rangle$ have quite similar numerical values, they are not strictly equal (they differ approximately by a factor 1.5). $\langle B \rangle$ represents the volume averaged magnetic field and B_0 is the proportionality factor in models (1−4), so that $B = B_0 \times f(\rho)$, where $f(\rho)$ is dimensionless. The particles are emitted from 10 different sources chosen randomly among regions of high baryonic density. A detailed description of our code is given in Appendix A of Kotera & Lemoine (2007).

Both plots of figure 3 illustrate the existence of a magnetic horizon for low energy extragalactic particles. Figure 3a shows the root mean square of the distance of 10^3 particles to their source after one Hubble time (13.9 Gyr) as a function of their energy, for a characteristic magnetic field $B_0 = 2$ nG and a coherence length $l_c = 300$ kpc. Our results are no longer valid beyond the dot-dashed line which represents the threshold energy above which the energy loss time becomes $\leq t_{\rm H}/2$, as our simulations do not compute energy losses. One notices immediately that particles of energy below $E \sim 3 \times 10^{17}$ eV cannot travel farther than a distance of a hundred megaparsecs from their sources. This corroborates the scenario of Lemoine (2005) and Aloisio & Berezinsky (2005) on the existence of a magnetic horizon, and extends it to the case of a inhomogeneous magnetic field.

In figure 3b, the transmission factor is plotted as a function of particle energy for three distances to the source (dashed lines: 10 Mpc, solid lines: 100 Mpc, dotted lines: 300 Mpc). Given an initial source position, we propagate protons over one Hubble time. At a distance R from the source, we calculate the transmission factor by taking the ratio between the number of particles situated beyond R and the total number of particles that were emitted. Again, the magnetic horizon effect is striking: for energies below $\sim 2 \times 10^{17}$ eV, only half of the emitted particles reach a distance of 100 Mpc in a Hubble time. Thin lines represent the analytical transmission factors calculated in Kotera & Lemoine (2007), for a homogeneous case. Unlike for the parameters of figure 3a, for the isotropic collapse model (model 1) and the represented parameters ($B_0 = 2$ nG, $l_{\rm c} = 100$ kpc), there is a noticeable difference between the homogeneous and the inhomogeneous cases. The cut-off occurs at lower energy for the inhomogeneous case, probably due to voids that enable particles to travel farther. This remark

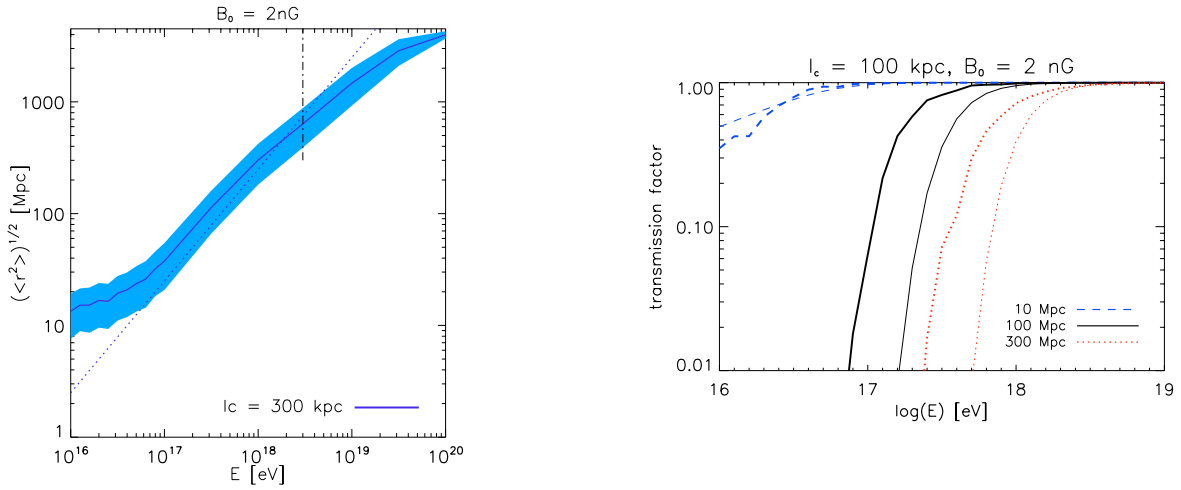

Fig. 2. (a) *Left:* Root mean square of the distance of 10^3 particles to their source after one Hubble time ($t_{\rm H} \sim 13.9$ Gyr) as a function of their energy, for $B_0 = 2$ nG and $l_c = 300$ kpc. The solid line represents the root mean square of the distance and the surrounding color band its variance. The dotted line shows the values obtained from analytical calculations in a homogeneous magnetic field and the dot-dashed line the threshold energy above which the energy loss time becomes $\leq t_{\rm H}/2$. (b) *Right:* Particle transmission factor at various distances from the source, as a function of particle energy. Thick lines are results from the simulation run with $B_0 = 2$ nG and $l_{\rm c} = 100$ kpc. Thin lines represent the analytical transmission factor for a homogeneous magnetic field.

does not stand for a travelled distance of 10 Mpc (blue dashed lines), due to dense environment effects.

In order to compare our results with observational data, we derive spectra from our simulations using the method described in Lemoine (2005). The extragalactic spectra are calculated separately for diffusive and rectilinear regimes, taking into account the evolution of the diffusion coefficient D, according to the redshift z, the mean magnetic field intensity $B_0(z)$ and the coherence length of the field $l_c(z)$ (for more details, see Kotera & Lemoine 2005). The galactic cosmic ray component is modeled as explained in Lemoine (2005).

In figure 3 we present the total spectra (galactic+extragalactic) compared to the data, for our parameter fit for each model. We draw the median spectrum (dot-dashed line) obtained over 100 realisations of the source locations. The upper and lower dotted curves show the $75^{\rm th}$ and $25^{\rm th}$ percentiles around this prediction, meaning that only 25% of spectra are higher or lower respectively than indicated by the curves. This uncertainty is related to the location of the closest sources. As explained in Lemoine (2005), we draw a straight dashed line in the region slightly above 10^{18} eV, where the propagation is neither rectilinear nor diffusive.

We use the data of six major experiments that measured the cosmic ray fluxes in our regions of interest: KASKADE (2004 data), with an energy range going from 10^{15} to 10^{17} eV, Akeno from 10^{15} to $10^{18.6}$ eV, AGASA from $10^{18.5}$ to $10^{20.5}$ eV, HiRes I and II from $10^{17.3}$ to 10^{20} eV and Fly's Eyes from $10^{17.3}$ to 10^{20} eV. We split these data in two sets in order to account for the discrepancy between HiRes and AGASA. This enables us to have two different normalizations for the extragalactic flux on the left and right panels. The normalization of KASKADE data remains the same for both sets.

Four main points emerge from Fig. 3. *(i)* The second knee feature appears more or less clearly in the four models, but ultimately remains quite robust to model changes. *(ii)* However, the influence of the magnetic field intensity in voids is obvious: even with a source density of $n_{\rm s} = 10^{-6}$ Mpc^{-3}, the goodness of fit of model 3 with the observed spectra is only marginal. This situation is clearly improved in the other models, especially if we consider the uncertainty on the position of the closest sources. *(iii)* One might also notice that this last element has a considerable impact on the cut-off energy, much more than in the case of the homogeneous magnetic field of Lemoine (2005). This is due to the presence of the diffusive regime at the low energy tail. One can indeed observe in figure 3 the flat diffusive locus at low energies for model 1 (this is also the case for model 4). Phenomenologically, one understands that for these models, a slight change in the closest source distance can influence greatly the flux of low energy particles. *(iv)* Finally, comparing our plots for AGASA and HiRes data,

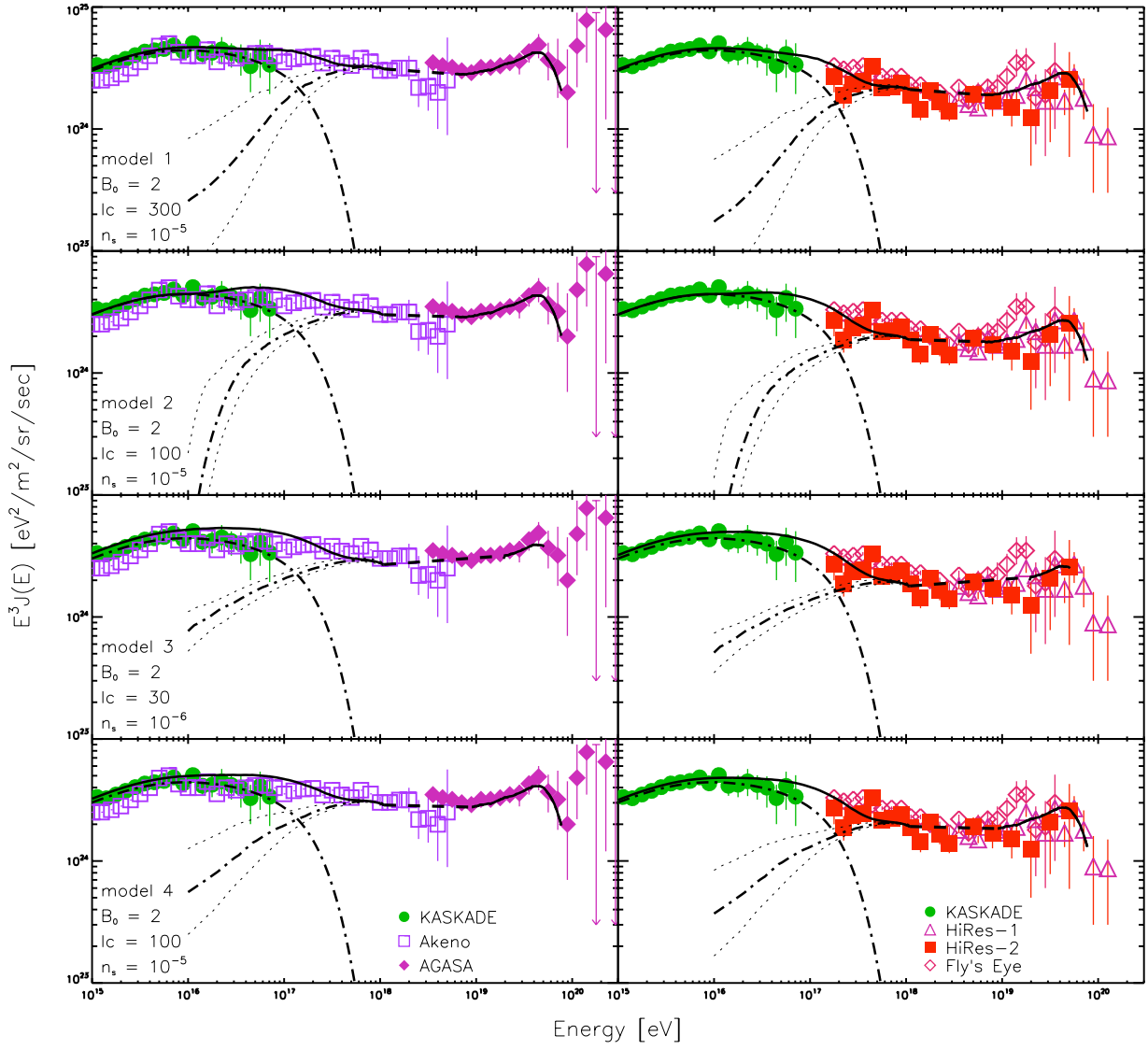

Fig. 3. Total spectra (galactic + extragalactic) compared to data. Each row corresponds to a model and a set of parameters. Caution: $n_s = 10^{-6}$ Mpc^{-3} for the third row. The left panels show KASKADE, Akeno and AGASA data. The right panels show KASKADE, HiRes-1, HiRes-2 and Fly's Eyes data. Solid lines represents the median values of the total flux, dot-dashed lines the separate galactic and extragalactic components and the dotted lines the upper 75$^{\text{th}}$ and lower 25$^{\text{th}}$ percentiles for the magnetic cut-off of the extragalactic flux.

we conclude that the fits are better for the latter. The higher slope above the second knee break point in the HiRes data as well as the gap of data between the KASCADE and HiRes ranges make the fitting easier.

4 Other signatures

We calculated the Faraday rotation measure (RM) for our four magnetic field models with a characteristic magnetic field of $B_0 = 2$ nG. We find that at a cosmological distance of 1 Gpc, the median of our RMs is of order ~ 0.03 rad/m^2 for model 1 and of ~ 0.1 rad/m^2 for models 2 and 3. These values are consistent with the current observations of RMs that predict an upper limit of 5 rad/m^2 (Kronberg 1994). It should be remarked however that the RMs calculated here are subject to high variations according to the concentration of matter

along the line of sight. Though the distribution of the RMs is sharply peaked around 0, with most of the RMs in the narrow interval of $[-0.5, 0.5]$ rad/m^2, we still find some punctual cases where the RM can diverge from 20 up to 2000 rad/m^2.

We also calculated the mean deflection angles for cosmological distances at high energy. For a particle energy of 5×10^{19} eV and a magnetic field of $B_0 = 2$ nG and $l_c = 300$ kpc, we find that the deflection is of order $\sim 3-5^o$ at 100 Mpc for models 1 and 2, and of $\sim 8^o$ for model 3. These results are consistent with the observations of doublets and triplets of events by recent experiments and leave room for doing cosmic ray astronomy. Our models would thus be in agreement with the detection of counterparts at energies around the GZK cut-off.

5 Conclusion

We developed a new method combining an efficient propagation scheme and a simple recipe to build semi-realistic magnetic field distributions. We map the magnetic field following the baryon density distribution according to three different models and propagate particles from cell to cell, taking into account the inner turbulence of each cell, as well as its global magnetic intensity. This method is much faster than classical trajectory integrations.

Under the assumption that the emergence of the extragalactic component occurs at the second knee, we demonstrated that it was possible give rough limits for some key parameters ($\langle B \rangle$, l_c), by studying their effects on the magnetic horizon.

For our models assuming isotropic or anisotropic collapse, with or without turbulence (models 1, 2 and 4 described in sections 2 and 3), we find that our calculated spectra fit the data satisfactorily. Numerically, for a source density of $n_s = 10^{-5}$ cm^{-3} we find that an average magnetic field $\langle B \rangle = 2$ nG is a reasonable value for the three models cited above, and coherence lengths of 100 kpc (for models 2 and 4) up to 300 kpc (model 1) provide a good agreement with the data. These numbers should still be taken cautiously, remembering the limitations discussed in this paper and in Kotera & Lemoine (2007).

We showed that the validity of this scenario depends on other parameters (relative normalisation of data sets, source density) but eventually, the strongest constraint comes from the rate of magnetic enrichment of the low density intergalactic medium (voids). We saw indeed that model 3, which simulates a volume with unmagnetized voids has a marginal goodness of fit with the observed spectra, even with a low source density.

Ultimately, therefore, the success of this scenario for the transition between the Galactic and extragalactic cosmic ray components depends on the very origin of intergalactic magnetic fields, and on whether the voids of large-scale structures have remained pristine or not. Interestingly, this question is related to the ongoing debate on the enrichment of the underdense intergalactic medium in metals, since galactic winds carrying metals also carry significant magnetic fields. Detailed studies of the intergalactic medium as well as progress on extragalactic magnetic fields in the coming decade will shed light on this issue.

References

AGASA collaboration: Takeda, M. et al. 1998, Phys. Rev. L, 81, 1163
Akeno collaboration: Nagano, M. et al. 1992, J. Phys. G, 18, 423
Aloisio, R., & Berezinsky, V. 2005, ApJ, 625, 249
Berezinsky, V., Gazizov, A., & Grigorieva, S. 2006, Phys. Rev. D, 74, 043005, arXiv: hep-ph/0204357
Casse, F., Lemoine, M., & Pelletier, G. 2002, Phys. Rev. D, 65, 023002
Dolag, K., Grasso, D., Springel, V., & Tkachev, I. 2005, JCAP, 1, 9
Fly's Eyes collaboration: Bird, D. J. et al. 1994, ApJ, 424, 491
Hires collaboration: Abbasi, R. U. et al. 2004, Phys. Rev. L, 92, 151101
KASKADE collaboration: Kampert, K.-H. et al. 2004, Acta Physica Polonica B, 35, 1799
Kotera, K., & Lemoine, M. 2007, arXiv:astro-ph/0706.1891
Kronberg, P. P. 1994, Rep. Prog. Phys., 57, 325
Lagage, P.-O., & Cesarsky, C. 1983, A&A, 125, L249
Lemoine, M. 2005, Phys. Rev. D, 71, 083007
Sigl, G., Miniati, F., & Ensslin, T. A. 2004, Phys. Rev. D, 70, 043007